HHS Public Access

Author manuscript

J Am Coll Cardiol. Author manuscript; available in PMC 2020 June 04.

Published in final edited form as:

J Am Coll Cardiol. 2019 June 04; 73(21): 2705–2718. doi:10.1016/j.jacc.2019.02.074.

Osteopontin Promotes Left Ventricular Diastolic Dysfunction through a Mitochondrial Pathway

Keyvan Yousefi, Pharm.D.[#,a,b], **Camila I. Irion, Ph.D.**[#,b,c], **Lauro M. Takeuchi, D.D.S.**[b], **Wen Ding, Ph.D.**[a,b], **Guerline Lambert, M.S.**[b,c], **Trevor Eisenberg, B.S.**[c], **Sarah Sukkar, B.S.**[c], **Hendrikus L. Granzier, Ph.D.**[d], **Mei Methawasin, M.D., Ph.D., B.S.**[d], **Dong I. Lee, Ph.D.**[e], **Virginia Hahn, M.D.**[e], **David A. Kass, M.D.**[e], **Konstantinos E. Hatzistergos, Ph.D.**[b,f], **Joshua M. Hare, M.D.**[b,c], **Keith A Webster, Ph.D.**[a,g], and **Lina A. Shehadeh, Ph.D.**[*,b,c,g,h]

[a]Department of Molecular and Cellular Pharmacology, University of Miami Leonard M. Miller School of Medicine, Miami, Florida;

[b]Interdisciplinary Stem Cell Institute, University of Miami Leonard M. Miller School of Medicine, Miami, Florida

[c]Department of Medicine, Division of Cardiology, University of Miami Leonard M. Miller School of Medicine, Miami, Florida, USA.

[d]Department of Cellular and Molecular Medicine, University of Arizona, Tucson, AZ

[e]Division of Cardiology, Department of Medicine, Johns Hopkins University, Baltimore, Maryland, USA

[f]Department of Cell Biology, University of Miami Leonard M. Miller School of Medicine, Miami, Florida, USA.

[g]Vascular Biology Institute, University of Miami Leonard M. Miller School of Medicine, Miami, Florida, USA.

[h]Peggy and Harold Katz Family Drug Discovery Center, University of Miami Leonard M. Miller School of Medicine, Miami, Florida

Abstract

Background: Patients with chronic kidney disease (CKD) and coincident heart failure with preserved ejection fraction (HFpEF) may constitute a distinct HFpEF phenotype. Osteopontin (OPN) is a biomarker of HFpEF and predictive of disease outcome. We recently reported that OPN

[*]**Corresponding Author:** Lina A. Shehadeh, PhD, Interdisciplinary Stem Cell Institute, University of Miami Leonard M. Miller School of Medicine, 1501 NW 10th Ave, Biomedical Research Building Rm 818, Miami, Florida 33136, Telephone: 305-243-0867, Fax: 305-243-3906, LShehadeh@med.miami.edu, Twitter: @umiamimedicine.
[#]These two authors contributed equally.

Disclosures: Dr. Lina Shehadeh and the University of Miami hold a pending patent on treatment of Alport Syndrome by targeting Osteopontin. All other co-authors have nothing to disclose.

blockade reversed hypertension, mitochondrial dysfunction and kidney failure in *Col4a3*$^{-/-}$ mice, a model of human Alport Syndrome.

Objectives: Identify potential OPN targets in biopsies of HF patients, healthy controls and human induced pluripotent stem cell-derived cardiomyocytes (hiPS-CMs). Characterize the cardiac phenotype of *Col4a3*$^{-/-}$ mice, relate this to HFpEF and investigate possible causative roles for OPN in driving the cardiomyopathy.

Methods: Ogdhl mRNA and protein were quantified in myocardial samples from patients with HFpEF, HFrEF, and donor controls. OGDHL expression was quantified in hiPS-CMs treated ± anti-OPN antibody. Cardiac parameters were evaluated in *Col4a3*$^{-/-}$ mice with and without global OPN knockout or AAV9-mediated delivery of 2-Oxoglutarate Dehydrogenase-Like (Ogdhl) to the heart.

Results: Ogdhl mRNA and protein displayed abnormal abundances in cardiac biopsies of HFpEF (N = 17) compared with donor controls (N = 12; $p < 0.01$) or HFrEF patients (N = 12; $p < 0.05$). Blockade of OPN in hiPS-CMs conferred increased OGDHL expression. *Col4a3*$^{-/-}$ mice demonstrated cardiomyopathy with similarities to HFpEF including diastolic dysfunction, cardiac hypertrophy and fibrosis, pulmonary edema, and impaired mitochondrial function. The cardiomyopathy was ameliorated by *Opn*$^{-/-}$ coincident with improved renal function and increased expression of Ogdhl. Heart-specific overexpression of Ogdhl in *Col4a3*$^{-/-}$ mice also improved cardiac function and cardiomyocyte energy state.

Conclusions: *Col4a3*$^{-/-}$ mice present a model of HFpEF secondary to CKD wherein OPN and OGDHL are intermediates, and possibly therapeutic targets.

Condensed Abstract:

Abnormal OGDHL expression was observed in cardiac biopsies of HFpEF patients compared to healthy donor or HFrEF groups. OGDHL levels were responsive to OPN activity in hiPS-CMs and rodent CMs. Cardiac structure and function analyses of Alport (*Col4a3*$^{-/-}$) mice that model monogenic kidney disease revealed, in addition to hypertension and renal dysfunction, a HFpEF-like phenotype that included pulmonary edema, diastolic dysfunction, cardiac hypertrophy, myocardial fibrosis and mitochondrial dysfunction. We identify pivotal roles for OPN and mitochondrial OGDHL in the pathophysiology and show that cardiac-specific overexpression of Ogdhl alleviated cardiac dysfunction and improved energetics, similar to global OPN knockdown.

Keywords

HFpEF; Alport Syndtome; hiPS-CM; Osteopontin; mitochondria; OGDHL

Introduction

Heart failure with preserved ejection fraction (HFpEF) is a complex and increasingly prevalent syndrome accounting for more than 50% of all HF cases (1,2). Relative to HF with reduced ejection fraction (HFrEF), HFpEF is more prevelant in the elderly and more commonly associated with, and possibly driven by co-morbidities including systemic hypertension, obesity, diabetes mellitus, chronic kidney disease, and coronary artery and microvascular diseases (3–7). Because of the heterogeneous nature of HFpEF and its diverse

underlying etiologies, pharmacological strategies including neurohumoral inhibition that are successfully used to treat HFrEF have not shown efficacy in large clinical trials of HFpEF (8–13). Rather it is proposed that more personalized treatment strategies are required that are tailored to individual HFpEF-specific signaling and phenotypic diversity as reflected by patient presentation and predisposition (1).

Epidemiological analyses suggest that patients with HFpEF in the presence of renal dysfunction represent a distinct phenotype (14,15). Consistent with this, phenomapping studies identified patients with chronic kidney disease (CKD), electrical and myocardial remodeling, pulmonary hypertension, and RV dysfunction as a subset of HFpEF patients that are at high clinical risk relative to other phenomapped groups (1). Animal models that accurately reproduce the clinical symptoms of different HFpEF subsets would be valuable to identify signaling intermediates and test for safety and efficacy of phenotype-specific interventions.

Recently we presented evidence that the pro-inflammatory cytokine Osteopontin (OPN) plays a causal role in the progression of CKD in Alport (*Col4a3*$^{-/-}$) mice, a model of autosomal Alport syndrome (16). Genetic disruption of the OPN gene in Alport mice ameliorated CKD and reversed systemic hypertension and mitochondrial dysfunction (16). Other work including our own described causal roles for OPN in cardiovascular disease and heart failure in humans and animal models where it has been labeled a “remodeling-specific marker” (17–21). Plasma levels of OPN are increased in HFpEF patients and predict outcome (22,23).

Here we establish that *Col4a3*$^{-/-}$ mice recapitulate multiple features of HFpEF, phenotypes that are ameliorated by targeting OPN. Alport mice may represent a subset of HFpEF patients wherein CKD is a primary cause of HF.

Methods

Animals

Animal procedures were approved by the University of Miami IACUC. *Col4a3*$^{-/-}$ mice on 129X1/SvJ background were from Jackson Lab and inter-bred with C57Bl/6 (*Opn*$^{-/-}$) and BALB/c mice at least 10 times as described previously (16). 129J mice were used to validate the HFpEF cardiac phenotypes. Disease progression in *Col4a3*$^{-/-}$ mice is highly dependent on genetic strain (24). Therefore, we used the 129X1/SvJ strain for invasive hemodynamic studies, AAV9-Ogdhl gene therapy, and titin isoform expression. Equal gender numbers were used.

Experimental procedures and statistical analyses are described in detail in the Online Appendix.

Results

Col4a3$^{-/-}$ mice develop diastolic dysfunction with preserved ejection fraction, impaired strain and pulmonary congestion

We recently reported that *Col4a3*$^{-/-}$ mice develop systemic hypertension(16). To examine cardiac function in *Col4a3*$^{-/-}$ mice, echocardiography and 2D-speckle tracking was implemented on 2-month old mixed genetic background animals and compared with wild type and *Opn*$^{-/-}$ littermates (16). Echocardiography revealed LV diastolic dysfunction of *Col4a3*$^{-/-}$ hearts. Isovolumetric relaxation time (IVRT) was prolonged from 16.4±1.27 ms in wild type to 25.69±1.71 ms in *Col4a3*$^{-/-}$ mice ($p<0.0001$), indicating impaired LV relaxation in *Col4a3*$^{-/-}$ mice (Figure 1A). Additionally, we found significantly increased early trans-mitral flow velocity to early mitral annulus velocity ratio (E/E') from 28.47±1.4 to 40.1±2.84 ($p<0.001$) in the *Col4a3*$^{-/-}$ mice (Figure 1B and Online Figure 1). Increased E/E' indicates elevated LV filling pressure and pulmonary artery wedge pressure (PCWP). The E/A ratio (early to late ventricular filling velocities) was also significantly reduced corroborating impaired LV relaxation in *Col4a3*$^{-/-}$ mice ($p<0.01$, Figure 1C). The myocardial performance index (MPI), also known as the Tei index was increased in *Col4a3*$^{-/-}$ mice by 63% compared to the wild type mice ($p<0.01$) (Figure 1D). The Tei index is inversely related to function consistent with elevated Tei indices reported in HFpEF patients (25).

Myocardial strain analyses revealed altered myocardial deformation in *Col4a3*$^{-/-}$ mice via impaired global longitudinal strain (GLS; −19.70±1.31 % in wild type versus −15.24±1.88 % in *Col4a3*$^{-/-}$ mice, $p<0.05$) and global circumferential strain (GCS; −23.52±1.03 % in wild type versus −18.23±1.24 % in *Col4a3*$^{-/-}$ group, $P<0.01$) as shown in Figure 1E–F, reflecting subclinical systolic dysfunction. This finding is also consistent with the subclinical systolic dysfunction reported in HFpEF patients (26). In addition, maximum opposing wall delay was increased in *Col4a3*$^{-/-}$ hearts, indicating asynchrony (Online Table 1). *Col4a3*$^{-/-}$ mice did not show significantly decreased EF, Cardiac Output or Stroke Volume (Figure 1G and Online Table 1). *Col4a3*$^{-/-}$ mice showed a significant increase in normalized lung weight, as well as lung wet-to-dry weight ratio consistent with pulmonary congestion, and suggesting congestive heart failure (Figure 1H–I; $p<0.01$). Complete echocardiographic and morphometric measurements are presented in Online Tables 1 and 2.

Col4a3$^{-/-}$ mice develop cardiac hypertrophy and fibrosis

Cardiac hypertrophy is common in HFpEF patients; therefore, we quantified cardiac dimensions in *Col4a3*$^{-/-}$ mice. Echocardiographic measurements revealed significantly increased relative wall thickness, LV anterior wall thickness, and interventricular septum thickness, ($p<0.05$, Online Table 1) indicating gross hypertrophy. Additionally, wheat germ agglutinin (WGA) staining confirmed increased myocyte cross-sectional area in *Col4a3*$^{-/-}$ mice compared to controls ($p<0.001$, Figure 2A–B). We next evaluated fibrosis, a major contributor to HFpEF. Picrosirius Red staining demonstrated a 4.2-fold increase in collagen content of *Col4a3*$^{-/-}$ hearts compared to wild type controls ($p<0.001$; Figure 2C–D). In addition, incorporation of EdU, by Myosin Light Chain 2 (MLC2)-negative interstitial cells was significantly upregulated (Fig 2E–F) suggesting fibroblast proliferation. Likewise, the

number of activated fibroblasts, as indicated by increased area of rough endoplasmic reticulum and collagen deposition, was increased (Electron Microscopy/EM; Figure 2G). These data establish the presence of cardiac hypertrophy and fibrosis in *Col4a3*$^{-/-}$ mice.

OPN deficiency in Col4a3$^{-/-}$ mice ameliorates cardiac dysfunction and prevents hypertrophy and fibrosis—OPN is elevated in the circulation of HFpEF patients and predicts outcome [22,23]. We recently reported that *Col4a3*$^{-/-}$ mice have increased renal and plasma levels of OPN (16). OPN is not upregulated in the hearts of *Col4a3*$^{-/-}$ mice. To investigate the effects of OPN downregulation, *Col4a3*$^{-/-}$ mice with homozygous and heterozygous deletion of OPN were subjected to cardiac functional and histological analyses. We found significant improvement in cardiac function and remodeling in *Col4a3*$^{-/-}$ mice with OPN deficiency. OPN deletion ameliorated diastolic function by restoring IVRT, E/E', E/A, and Tei index (Figure 1A–D). Moreover, *Col4a3*$^{-/-}$ mice on hetero- or homo-zygous OPN knockout backgrounds showed normal myocardial wall thickness (Online Table 1) and myocyte cross-sectional area (Figure 2A–B). OPN deficiency markedly decreased myocardial fibrosis in *Col4a3*$^{-/-}$ mice as shown by Picrosiurius Red staining (Figure 2C–D and Online Figure 2), reduced Edu incorporation in interstitial cells (Figure 2E–F), and reduced collagen fibers and interstitial "activated" fibroblasts (Figure 2G).

Dysregulated Ogdhl in Col4a3$^{-/-}$ hearts—Gene microarray analysis were implemented on total RNA isolated from hearts of 2-month wild type, *Col4a3*$^{-/-}$ and *Col4a3*$^{-/-}$*Opn*$^{-/-}$ mice (n = 3 per group). We identified 19 differentially expressed genes, of which 3 were up-regulated and 16 downregulated (Figure 3A; Online Table 3). Quantitative real-time PCR (qPCR) results confirmed that the expression of Hbb-b1, Alas2, Cnn1, Aqp7 and Ogdhl genes was significantly lower in *Col4a3*$^{-/-}$ hearts. In addition to mRNA expression, OGDHL protein levels were decreased in total homogenate and mitochondrial fractions of *Col4a3*$^{-/-}$ hearts (Figure 3C–D) but increased in *Col4a3*$^{-/-}$*Opn*$^{-/-}$ double knockouts (Figure 3F). OGDH enzymatic activity was also significantly lower in extracts from *Col4a3*$^{-/-}$ hearts (Figure 3E). These data suggest that OGDHL regulation by OPN contributes to the cardiac pathology of *Col4a3*$^{-/-}$ mice.

Increased oxidative stress and loss of mitochondrial integrity in Col4a3$^{-/-}$ hearts—To further explore abnormalities in energy transduction we investigated mitochondrial morphology and function in *Col4a3*$^{-/-}$ hearts. Elevated oxidative stress including depressed redox state and elevated lipid peroxidation is common in HF. We found that oxidative stress was markedly elevated in *Col4a3*$^{-/-}$ hearts, including 50% reduction in GSH:GSSG ratio (Online Figure 3A) and 35% increase in the levels of malondialdehyde (MDA, Online Figure 3B). We also found significant reductions in the levels of the mitochondrial electron transport chain Complexes I, II and IV ($p<0.05$, Online Figure 3C). EM revealed dysmorphic mitochondria that were swollen with disorganized cristae in *Col4a3*$^{-/-}$ hearts (Online Figure 3D). Such features of oxidative stress and mitochondrial dysfunction are common in HF patients and animal models (27–29).

Negative regulation of Ogdhl and mitochondria by OPN—To further investigate functional interactions between OPN and OGDHL we developed a monoclonal antibody against human OPN (OPN mAb). OGDHL protein was quantified in hiPS-CMs after treatment for 24h with OPN mAb. Immunostaining and western blots showed that neutralization of OPN conferred significant increases in OGDHL (Figure 4A–C). In addition, we found that treating mouse neonatal cardiomyocytes (nCMs) with recombinant OPN protein for 48 hours significantly suppressed ATP-linked oxygen consumption (Figure 4D–E). These data are consistent with negative regulation of Ogdhl and mitochondrial respiration by OPN.

Validation of diastolic dysfunction in Col4a3$^{-/-}$ on 129J background—In order to validate the HFpEF cardiac phenotype of mixed background mice in pure 129J background, the experiments were repeated on *Col4a3*$^{-/-}$ 129J mice. In contrast to the gross and cellular hypertrophy seen in *Col4a3*$^{-/-}$ on a mixed background, *Col4a3*$^{-/-}$ 129J mice did not demonstrate such hypertrophy (Online Table 4). This finding is consistent with previous reports (30,31). However, both echocardiography and invasive hemodynamic measurements confirmed diastolic dysfunction in *Col4a3*$^{-/-}$ 129J mice similar to the mixed background results. As shown in Figure 5A–B, *Col4a3*$^{-/-}$ 129J mice had significantly prolonged IVRT and markedly increased Tei indices. However, the *Col4a3*$^{-/-}$ 129J mice displayed a more compromised systolic function than the mixed background mice. While EFs were not reduced (Figure 5C), *Col4a3*$^{-/-}$ 129J mice showed significantly decreased cardiac output and stroke volume (Figure 5D–E), $p<0.05$). Moreover, strain analysis in *Col4a3*$^{-/-}$129J mice also indicated myocardial deformation shown by impaired GLS and GCS (Figure 5 F–G), similar to the mixed strain line. Complete echocardiographic and morphometric measurements are presented in Online Tables 4 and 5.

Invasive LV catheterization revealed markedly increased end-diastolic pressure-volume relationship (EDPVR, Figure 6B $p<0.01$), prolonged time constant of LV relaxation (Tau, Figure 6C, $p<0.01$) and significantly increased dP/dt_{min} (Figure 6D, $p<0.05$), each supporting diastolic dysfunction. Moreover, LV end-diastolic pressure (LVEDP) was increased from 4.6±0.3 in wild type mice to 8.63±1.01 in the *Col4a3*$^{-/-}$ 129J group (Figure 6E, $p<0.01$), corroborating elevated LV filling pressures. Complete invasive hemodynamics measurements are presented in Online Table 6.

While increased upregulation of titin N2BA isoform was reported in some HFpEF patients as a compensatory response to increased myocardial stiffness (32), it was absent in others (33). We detected no significant changes of titin isoforms in the LV of *Col4a3*$^{-/-}$ hearts (Online Figure 4).

AAV9-Ogdhl gene therapy in Col4a3$^{-/-}$ mice ameliorates cardiac dysfunction —We performed Ogdhl gene delivery to *Col4a3*$^{-/-}$ hearts using heart-specific AAV9-cTnT-Ogdhl and AAV9-cTnT-Luciferase as control. *Col4a3*$^{-/-}$ 129J mice at 4-weeks received single tail vein injections of AAV vectors (1×10^{12} vg/mouse) and gene delivery was confirmed by IVIS imaging, qPCR and western blot after an additional 4 weeks (Online Figure 5). Cardiac function was analyzed in parallel by echocardiography. Although Ogdhl overexpression did not change the prolonged IVRT (Figure 5A), the myocardial

performance index (MPI) was significantly reduced relative to un-injected or Luciferase-injected controls (Figure 5B). Moreover, Ogdhl overexpression markedly improved GLS (Figure 5F) relative to un-injected or Luciferase-injected controls, suggesting that gene therapy improved cardiac systolic function. *Col4a3*$^{-/-}$ mice that underwent gene therapy also demonstrated significantly higher body weights relative to un-injected controls suggesting a generally improved physiology (Figure 5H). Complete echocardiographic and morphometric measurements are presented in Online Tables 4 and 5.

Compromised mitochondrial respiration is rescued by Ogdhl gene therapy— To directly assess myocardial mitochondrial respiration in *Col4a3*$^{-/-}$ hearts ± Ogdhl, Seahorse XF assays were performed on adult cardiac myocytes 4 weeks after AAV9 delivery. We found that over-expression of Ogdhl in *Col4a3*$^{-/-}$ mice significantly improved mitochondrial function (Fig 5I–J). These results support our hypothesis that cardioprotection conferred by OPN deficiency in *Col4a3*$^{-/-}$ hearts is mediated at least in part through Ogdhl elevation and enhanced energy metabolism.

OGDHL expression is dysregulated in cardiac biopsies of HF patients—To determine whether mitochondrial functions and Ogdhl were similarly compromised in the clinical setting, we quantified Ogdhl transcript and protein levels in cardiac biopsies from patients with HFpEF, HFrEF and donor controls. Demographics of the patients are summarized in Table 1. Unexpectedly, we found that transcript levels of Ogdhl were significantly higher in samples from both HFpEF and HFrEF compared with healthy controls whereas OGDHL protein was elevated only in the HFpEF group (Figure 7). While these results do not support suppression of the Ogdhl gene as a general mechanism underlying global bioenergetic dysfunction during HF, they do suggest that this pathway is dysregulated in both HF groups relative to controls. It should be noted that obesity and diabetes were underlying co-morbidities of the HFpEF group relative to controls or HFrEF, and these may influence bioenergetic signaling pathways including Ogdhl expression. Therefore, the HFpEF phenotype of this group may be distinct from that driven primarily by CKD in patients or Alport mice.

Discussion

Cardiac phenotype of Col4a3$^{-/-}$ mice

We show that Alport (*Col4a3*$^{-/-}$) mice at age 2-months reproduce multiple phenotypes of HFpEF that were significantly ameliorated by genetic disruption of the OPN gene. Alport mice displayed diastolic dysfunction with preserved EF, myocardial deformation, hypertrophy, fibrosis, pulmonary edema, and mitochondrial dysfunction. Others and ourselves have previously reported on the renal insufficiency and systemic hypertension in these mice both of which are also significantly ameliorated by OPN deficiency (16,30). Despite their preserved EFs, *Col4a3*$^{-/-}$ mice displayed myocardial deformation as indicated by impaired GLS and GCS that is suggestive of the subclinical systolic dysfunction often seen in human HFpEF (26,34).

Role of Osteopontin in driving a HFpEF-like phenotype

Col4a3$^{-/-}$ animals with OPN hetero- or homozygous deletion presented a much more neutral cardiac phenotype with improved diastolic function and decreased myocardial hypertrophy and fibrosis. Microarray analysis identified multiple down-regulated, energetics-related genes in *Col4a3*$^{-/-}$ hearts that were rescued by OPN deficiency. Of these, 2-Oxo-Glutarate Dehydrogenase-like (OGDHL), a mitochondrial protein involved in metabolic substrate fluxes and signaling (35,36), displayed the most robust response. OGDHL mRNA, protein and enzyme activity were all substantially decreased in *Col4a3*$^{-/-}$ hearts, and OGHDL expression was rescued by OPN deficiency. *Col4a3*$^{-/-}$ mice displayed dysmorphic and dysfunctional cardiac mitochondria with evidence of increased oxidative stress. These defects were also absent in OPN deficient *Col4a3*$^{-/-}$ mice. Roles for OPN in disruption of mitochondrial functions in the model was further supported by our *in vitro* studies on isolated cardiac myocytes from mice or hiPS-CMs as well as by Ogdhl gene therapy *in vivo*. OPN reduced mitochondrial function of cultured cardiac myocytes and cardiac-specific overexpression of Ogdhl in *Col4a3*$^{-/-}$ hearts reversed the mitochondrial defects. Notably, Ogdhl gene therapy conferred significant improvements of cardiac systolic function, strain, and bioenergetics, consistent with a central role for OPN-induced mitochondrial dysfunction in promoting a HFpEF-like cardiac phenotype in this model.

OGDHL protein levels were increased in cardiac biopsies of HFpEF patients. Depressed OGDHL activity has been associated with neuronal degradation (37) and tumor growth (38), whereas up-regulation of the enzyme has been described in association with stress in the brain and heart (39). Therefore, dysregulation of OGDHL in either direction associated with pathological stress may contribute to CKD-related HFpEF. Further studies are required to fully define the relationships between OPN, OGDHL and HF and determine whether the OGDHL/OPN axis is a viable therapeutic target in different subsets of HFpEF patients. Whereas our cellular and gene therapy data showing induced expression of OGDHL by treatment of CMs with an OPN neutralizing antibody and partial reversal of cardiomyopathy by AAV9-Ogdhl (Figure 5) supports direct effects of OPN on OGDHL, we cannot rule out the possibility that global KO of OPN in this model confers a time-restricted cardioprotection by an as yet unidentified pathway(s).”

Do Col4a3$^{-/-}$ mice model a CKD subtype of HFpEF?

Impaired renal function is a risk factor for developing HFpEF (15,40). Therefore, we considered whether the Alport mouse models a CKD-HFpEF subset. Epidemiology studies indicate that a CKD-HFpEF subset of patients present with more LV hypertrophy, a larger LV systolic functional deficit, impaired left atrial mechanics and RV dysfunction (15). Our echocardiography and 2D-speckle tracking studies confirmed impaired LV relaxation, elevated LV filling and pulmonary artery wedge pressures, increased myocardial performance index and normal EF. Strain analyses confirmed myocardial deformation with impaired global longitudinal and circumferential strain reflecting mild systolic dysfunction. *Col4a3*$^{-/-}$ mice displayed global myocardial hypertrophy, fibrosis and pulmonary congestion consistent CHF. These changes are consistent with such a CKD-induced HFpEF phenotype. Shah et al recently proposed a personalized medical approach to the treatment of HFpEF wherein each specific phenotype is targeted by polypharmacology (1). Such an approach

may benefit from phenotype-specific animal models that could be used to test for safety and efficacy of such drug combinations. For example, *Col4a3*$^{-/-}$ mice could be used to test for safety and efficacy of combinations of diuretics, ACEI, ARBs, β-blockers, dobutamine, neprilysin inhibitors, and OPN antagonists (monoclonal antibody or aptamer).

In conclusion, *Col4a3*$^{-/-}$ mice reproduce a CKD-HFpEF-like phenotype that includes renal and diastolic dysfunction, myocardial deformation, hypertension, cardiac hypertrophy, pulmonary congestion, fibrosis and bioenergetic deficit. The phenotype is globally ameliorated by downregulation of OPN and the cardiac phenotype appears to be driven at least in part by OPN-mediated loss of mitochondrial enzymes including Ogdhl.

Limitations of our study include imperfect matching of the subset of the clinical HFpEF population (backgrounds of diabetes, obesity, and no data on serum OPN) with the preclinical model of CKD-related HFpEF. Similarly, while the human tissues were obtained from a similar region of the RV, the patients do have altered co-morbidity with greater obesity in the HFpEF subjects for example. Heart transplantation is generally restricted to a BMI <35, whereas many of our HFpEF patients have higher values. Donor hearts will not have this level of obesity or diabetes as seen in HFpEF. While some HFrEF patients had DM, it was not as common as in HFpEF. Donor hearts lacked these features by definition. In addition, left ventricle biopsies were taken from mice, although the anatomical mismatching may not be a major concern because in separate analyses, we did examine RV versus LV OGDHL protein expression in HFrEF and non-failing donors where we could obtain tissue from both ventricles from the same heart, and found them similar (Online Figure 6; Online Table 7).

Another limitation involves the short lifespan and severe nephropathy of the preclinical model. Finally, whereas bioenergetic perturbations involving mitochondrial Ogdhl are implicated by our HFpEF-Alport model studies, the discrepancy of OGDHL changes in human versus mouse samples leaves open the possibility that OPN confers its effects by as yet unidentified pathways possibly involving more global effects of the cytokine on heart and kidney function.

Supplementary Material

Refer to Web version on PubMed Central for supplementary material.

Acknowledgments.

We thank the Electron Microscope Core Facility and the Imaging Core Facility at the University of Miami Miller School of Medicine. The authors thank the invaluable contribution of Dr. Kavita Sharma, Director of the HFpEF Clinical Service at the Johns Hopkins University Hospital, who obtained all of the HFpEF endomyocardial biopsies that were analyzed for this study.

Funding. This work was supported by the following grants to LAS: National Institute of Health (R56HL132209 and 1R01HL140468) and the Miami Heart Research Institute. The NHLBI's Gene Therapy Resource Program (GTRP) funded the AAV generation at the Penn Vector Core. KY is a recipient of AHA predoctoral fellowship (18PRE33960070). WD is a recipient of a Sublett AHA predoctoral fellowship (15PRE22450019).

Abbreviations:

EDPVR	End-Diastolic Pressure-Volume Relationship
HFpEF	Heart Failure with Preserved Ejection Fraction
HFrEF	Heart Failure with Reduced Ejection Fraction
IVRT	Isovolumetric Relaxation Time
LVEDP	Left Ventricular End-Diastolic Pressure
LVEF	Left Ventricular Ejection Fraction
OGDHL	2-Oxoglutarate Dehydrogenase-Like
OPN	Osteopontin
hiPSCs	Human-induced pluripotent Stem Cells
CMs	Cardiac Myocytes

REFERENCES

1. Shah SJ, Kitzman DW, Borlaug BA et al. Phenotype-specific treatment of heart failure with preserved ejection fraction: a multiorgan roadmap. Circulation 2016;134:73–90. [PubMed: 27358439]
2. Lam CSP, Donal E, Kraigher-Krainer E, Vasan RS. Epidemiology and clinical course of heart failure with preserved ejection fraction. Eur J Heart Fail 2011;13:18–28. [PubMed: 20685685]
3. Bhatia RS, Tu JV, Lee DS et al. Outcome of heart failure with preserved ejection fraction in a population-based study. N Engl J Med 2006;355:260–269. [PubMed: 16855266]
4. Owan TE, Hodge DO, Herges RM, Jacobsen SJ, Roger VL, Redfield MM. Trends in Prevalence and Outcome of Heart Failure with Preserved Ejection Fraction. N Engl J Med 2006;355:251–259. [PubMed: 16855265]
5. Shah SJ, Gheorghiade M. Heart failure with preserved ejection fraction: treat now by treating comorbidities. JAMA 2008;300:431–433. [PubMed: 18647986]
6. Yancy CW, Lopatin M, Stevenson LW et al. Clinical presentation, management, and in-hospital outcomes of patients admitted with acute decompensated heart failure with preserved systolic function: a report from the Acute Decompensated Heart Failure National Registry (ADHERE) Database. J Am Coll Cardiol 2006;47:76–84. [PubMed: 16386668]
7. Fonarow GC, Stough WG, Abraham WT et al. Characteristics, treatments, and outcomes of patients with preserved systolic function hospitalized for heart failure: a report from the OPTIMIZE-HF Registry. J Am Coll Cardiol 2007;50:768–777. [PubMed: 17707182]
8. Holland DJ, Kumbhani DJ, Ahmed SH, Marwick TH. Effects of treatment on exercise tolerance, cardiac function, and mortality in heart failure with preserved ejection fraction. A meta-analysis. J Am Coll Cardiol 2011;57:1676–86. [PubMed: 21492765]
9. Yusuf S, Pfeffer MA, Swedberg K et al. Effects of candesartan in patients with chronic heart failure and preserved left-ventricular ejection fraction: the CHARM-Preserved Trial. Lancet 2003;362:777–81. [PubMed: 13678871]
10. Anand IS, Rector TS, Cleland JG et al. Prognostic value of baseline plasma amino-terminal pro-brain natriuretic peptide and its interactions with irbesartan treatment effects in patients with heart failure and preserved ejection fraction: findings from the I-PRESERVE trial. Circ Heart Fail 2011;4:569–77. [PubMed: 21715583]

11. Solomon SD, Claggett B, Lewis EF et al. Influence of ejection fraction on outcomes and efficacy of spironolactone in patients with heart failure with preserved ejection fraction. Eur Heart J 2016;37:455–62. [PubMed: 26374849]
12. Upadhya B, Brubaker PH, Morgan TM et al. The effect of Aliskiren on exercise capacity in older patients with heart failure and preserved ejection fraction: A randomized, placebo-controlled, double-blind trial. Am Heart J 2018.
13. Edelmann F, Musial-Bright L, Gelbrich G et al. Tolerability and Feasibility of Beta-Blocker Titration in HFpEF Versus HFrEF: Insights From the CIBIS-ELD Trial. JACC Heart failure 2016;4:140–149. [PubMed: 26682793]
14. Gori M, Senni M, Gupta DK et al. Association between renal function and cardiovascular structure and function in heart failure with preserved ejection fraction. Eur Heart J 2014;35:3442–51. [PubMed: 24980489]
15. Unger ED, Dubin RF, Deo R et al. Association of chronic kidney disease with abnormal cardiac mechanics and adverse outcomes in patients with heart failure and preserved ejection fraction. Eur J Heart Fail 2016;18:103–112. [PubMed: 26635076]
16. Ding W, Yousefi K, Goncalves S et al. Osteopontin deficiency ameliorates Alport pathology by preventing tubular metabolic deficits. JCI Insight 2018;3.
17. Li J, Yousefi K, Ding W, Singh J, Shehadeh LA. Osteopontin RNA aptamer can prevent and reverse pressure overload-induced heart failure. Cardiovasc Res 2017;113:633–643. [PubMed: 28453726]
18. Behnes M, Brueckmann M, Lang S et al. Diagnostic and prognostic value of osteopontin in patients with acute congestive heart failure. Eur J Heart Fail 2013;15:1390–1400. [PubMed: 23851388]
19. Singh K, Sirokman G, Communal C et al. Myocardial osteopontin expression coincides with the development of heart failure. Hypertension 1999;33:663–70. [PubMed: 10024324]
20. Philipp S, Florian B, Peter P et al. Increased myocardial expression of osteopontin in patients with advanced heart failure. Eur J Heart Fail 2002;4:139–146. [PubMed: 11959041]
21. Graf K, Do YS, Ashizawa N et al. Myocardial Osteopontin Expression Is Associated With Left Ventricular Hypertrophy. Circulation 1997;96:3063–3071. [PubMed: 9386176]
22. Krum H, Elsik M, Schneider HG et al. Relation of Peripheral Collagen Markers to Death and Hospitalisation in Patients with Heart Failure and Preserved Ejection Fraction: Results of the I-PRESERVE Collagen Sub-Study. Circ Heart Fail 2011.
23. Tromp J, Khan MA, Klip IT et al. Biomarker Profiles in Heart Failure Patients With Preserved and Reduced Ejection Fraction. J Am Heart Assoc 2017;6.
24. Kang JS, Wang XP, Miner JH et al. Loss of alpha3/alpha4(IV) collagen from the glomerular basement membrane induces a strain-dependent isoform switch to alpha5alpha6(IV) collagen associated with longer renal survival in Col4a3−/− Alport mice. J Am Soc Nephrol 2006;17:1962–9. [PubMed: 16769745]
25. Kim H, Yoon H-J, Park H-S et al. Usefulness of Tissue Doppler Imaging-Myocardial Performance Index in the Evaluation of Diastolic Dysfunction and Heart Failure With Preserved Ejection Fraction. Clin Cardiol 2011;34:494–499. [PubMed: 21780137]
26. Russo C, Jin Z, Elkind MSV et al. Prevalence and prognostic value of subclinical left ventricular systolic dysfunction by global longitudinal strain in a community-based cohort. Eur J Heart Fail 2014;16:1301–1309. [PubMed: 25211239]
27. Brown DA, Perry JB, Allen ME et al. Expert consensus document: mitochondrial function as a therapeutic target in heart failure. Nature Reviews Cardiology 2017;14:238. [PubMed: 28004807]
28. Bowen TS, Rolim NP, Fischer T et al. Heart failure with preserved ejection fraction induces molecular, mitochondrial, histological, and functional alterations in rat respiratory and limb skeletal muscle. Eur J Heart Fail 2015;17:263–272. [PubMed: 25655080]
29. Franssen C, Chen S, Unger A et al. Myocardial Microvascular Inflammatory Endothelial Activation in Heart Failure With Preserved Ejection Fraction. JACC: Heart Failure 2016;4:312–324. [PubMed: 26682792]
30. Neuburg S, Dussold C, Gerber C et al. Genetic background influences cardiac phenotype in murine chronic kidney disease. Nephrol Dial Transplant 2018;33:1129–1137. [PubMed: 29309658]

31. Touchberry CD, Green TM, Tchikrizov V et al. FGF23 is a novel regulator of intracellular calcium and cardiac contractility in addition to cardiac hypertrophy. American Journal of Physiology - Endocrinology and Metabolism 2013;304:E863–E873. [PubMed: 23443925]
32. Borbély A, Falcao-Pires I, Van Heerebeek L et al. Hypophosphorylation of the Stiff N2B titin isoform raises cardiomyocyte resting tension in failing human myocardium. Circ Res 2009;104:780–786. [PubMed: 19179657]
33. Zile MR, Baicu CF, Ikonomidis JS et al. Myocardial stiffness in patients with heart failure and a preserved ejection fraction: contributions of collagen and titin. Circulation 2015;131:1247–1259. [PubMed: 25637629]
34. Biering-Sørensen T, Solomon SD. Assessing Contractile Function When Ejection Fraction Is Normal: A Case for Strain Imaging. Circ Cardiovasc Imaging 2015;8.
35. Stobbe MD, Houten SM, van Kampen AH, Wanders RJ, Moerland PD. Improving the description of metabolic networks: the TCA cycle as example. FASEB J 2012;26:3625–36. [PubMed: 22661004]
36. Sen T, Sen N, Noordhuis MG et al. OGDHL Is a Modifier of AKT-Dependent Signaling and NF-κB Function. PLoS ONE 2012;7:e48770. [PubMed: 23152800]
37. Yoon WH, Sandoval H, Nagarkar-Jaiswal S et al. Loss of Nardilysin, a Mitochondrial Co-chaperone for alpha-Ketoglutarate Dehydrogenase, Promotes mTORC1 Activation and Neurodegeneration. Neuron 2017;93:115–131. [PubMed: 28017472]
38. Fedorova MS, Kudryavtseva AV, Lakunina VA et al. [Downregulation of OGDHL expression is associated with promoter hypermethylation in colorectal cancer]. Mol Biol. 2015;49:678–88.
39. Graf A, Trofimova L, Loshinskaja A et al. Up-regulation of 2-oxoglutarate dehydrogenase as a stress response. Int J Biochem Cell Biol 2013;45:175–89. [PubMed: 22814169]
40. Ter Maaten JM, Damman K, Verhaar MC et al. Connecting heart failure with preserved ejection fraction and renal dysfunction: the role of endothelial dysfunction and inflammation. Eur J Heart Fail 2016;18:588–598. [PubMed: 26861140]

CLINICAL PERSPECTIVES

Competency in Medical Knowledge:

The *Col4a3*$^{-/-}$ mouse exhibits several major pathological features of heart failure with preserved ejection fraction (HFpEF) associated with chronic kidney disease (CKD). In this model, blockade of osteopontin reversed hypertension, mitochondrial dysfunction and kidney failure.

Translational Outlook:

Further investigation is needed to determine if targeting specific regulators of myocardial energetics could favorably impact the clinical manifestations of HFpEF.

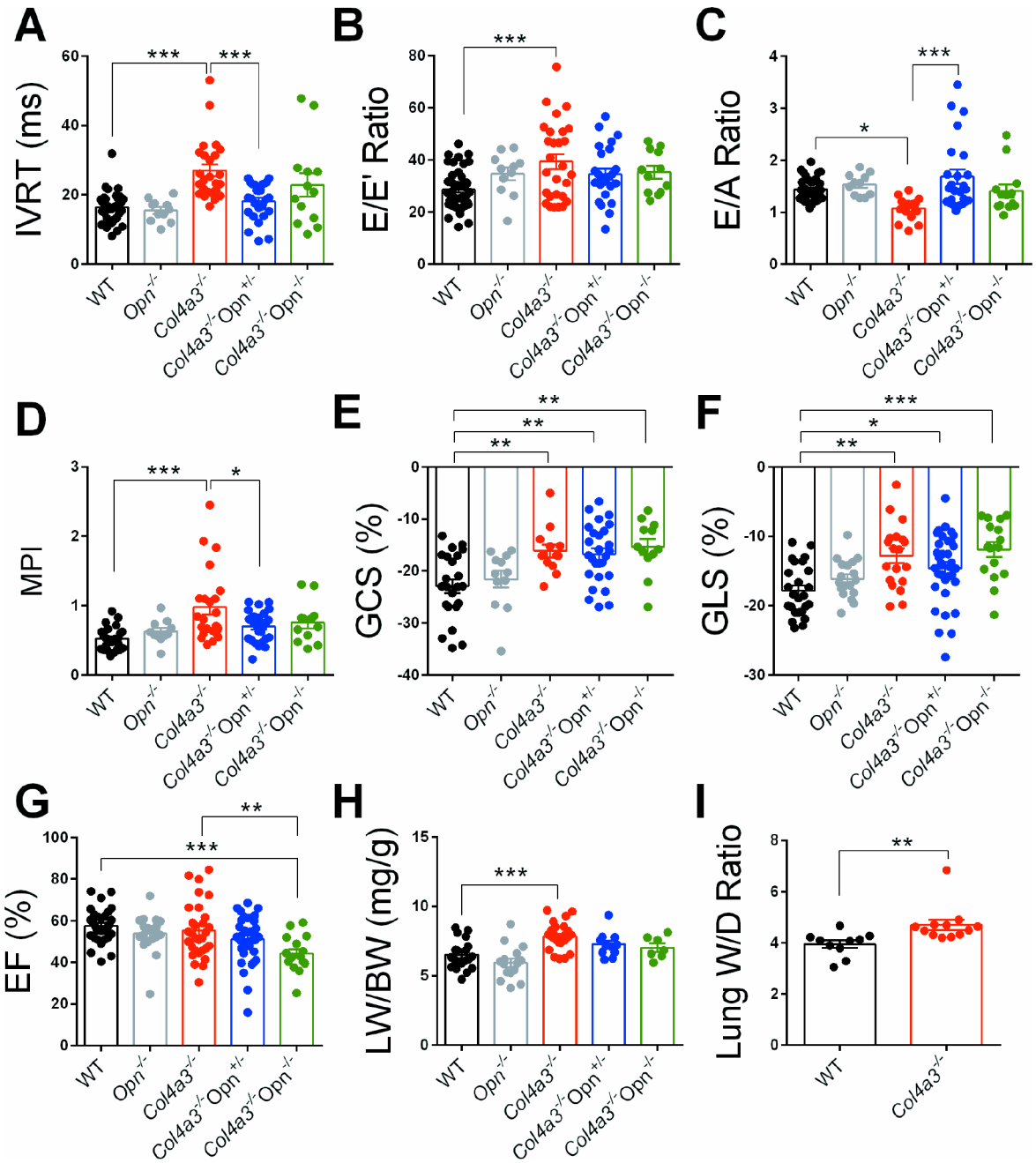

Figure 1: OPN deficiency ameliorates cardiac dysfunction in *Col4a3*$^{-/-}$ mice.

A-D. Echocardiography of 2-month *Col4a3*$^{-/-}$ mixed background mice shows diastolic dysfunction as indicated by a prolonged IVRT, increased E/E', reduced E/A, and elevated MPI. **E-F**. GLS and GCS were impaired in the *Col4a3*$^{-/-}$ mice indicating subclinical systolic dysfunction. **G** *Col4a3*$^{-/-}$ mice show preserved EF. **H.** Pulmonary edema is suggested by increased body weight-normalized lung weight as well as by elevated Lung wet-to-dry (W/D) ratio, indicating failing hearts in *Col4a3*$^{-/-}$ mice. Hetero-/homo-zygous deletion of OPN in *Col4a3*$^{-/-}$ mice improves cardiac function and prevents pulmonary edema. Complete echocardiographic and morphometric measurements are presented in

Online Tables 1 and 2. Data are mean±SEM. N=10–37 mice per group. *p<0.05, **p<0.01, ***p<0.001 using student's t-test for two groups (panel I) comparisons or one-way ANOVA with Tukey's post hoc test for multiple groups (all other panels).

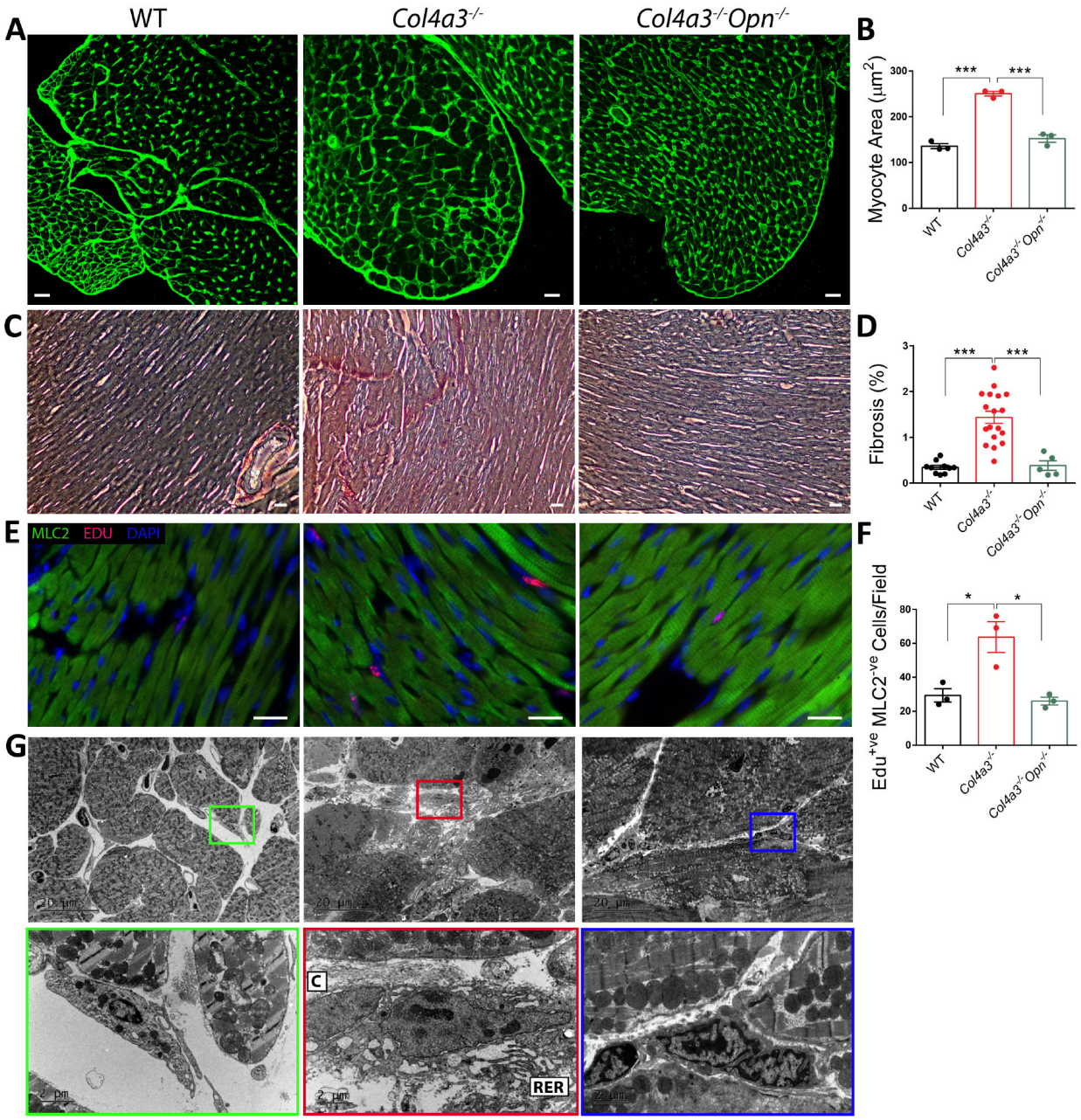

Figure 2: OPN deficiency ameliorates cardiac hypertrophy and fibrosis in *Col4a3*$^{-/-}$ mice.

A-B. WGA staining of *Col4a3*$^{-/-}$ hearts shows cardiac hypertrophy in *Col4a3*$^{-/-}$ mice as increased myocyte cross-sectional area that is reduced with OPN knockout. Scale bar: 20μm. N=3 mice per group. **C-D.** Picrosirius Red staining of cardiac cross-sections indicated increased Collagen deposition in *Col4a3*$^{-/-}$ heart that is significantly reduced by OPN deficiency. Scale bar: 100μm. N=5–15 mice per group. **E-F.** The number of Edu positive interstitial cells (MLC2 negative) is elevated in *Col4a3*$^{-/-}$ hearts but normalized with OPN deficiency Scale bar: 20μm. N=3 per mice group. **G.** OPN deficiency markedly decreased myocardial fibrosis in *Col4a3*$^{-/-}$ mice as shown by EM images of reduced collagen fibers and interstitial “activated” fibroblasts. C: Collagen fibers, RER: Rough Endoplasmic

Reticulum. Data are mean±SEM. *p<0.05, **p<0.01, ***p<0.001 using one-way ANOVA with Tukey's post hoc test.

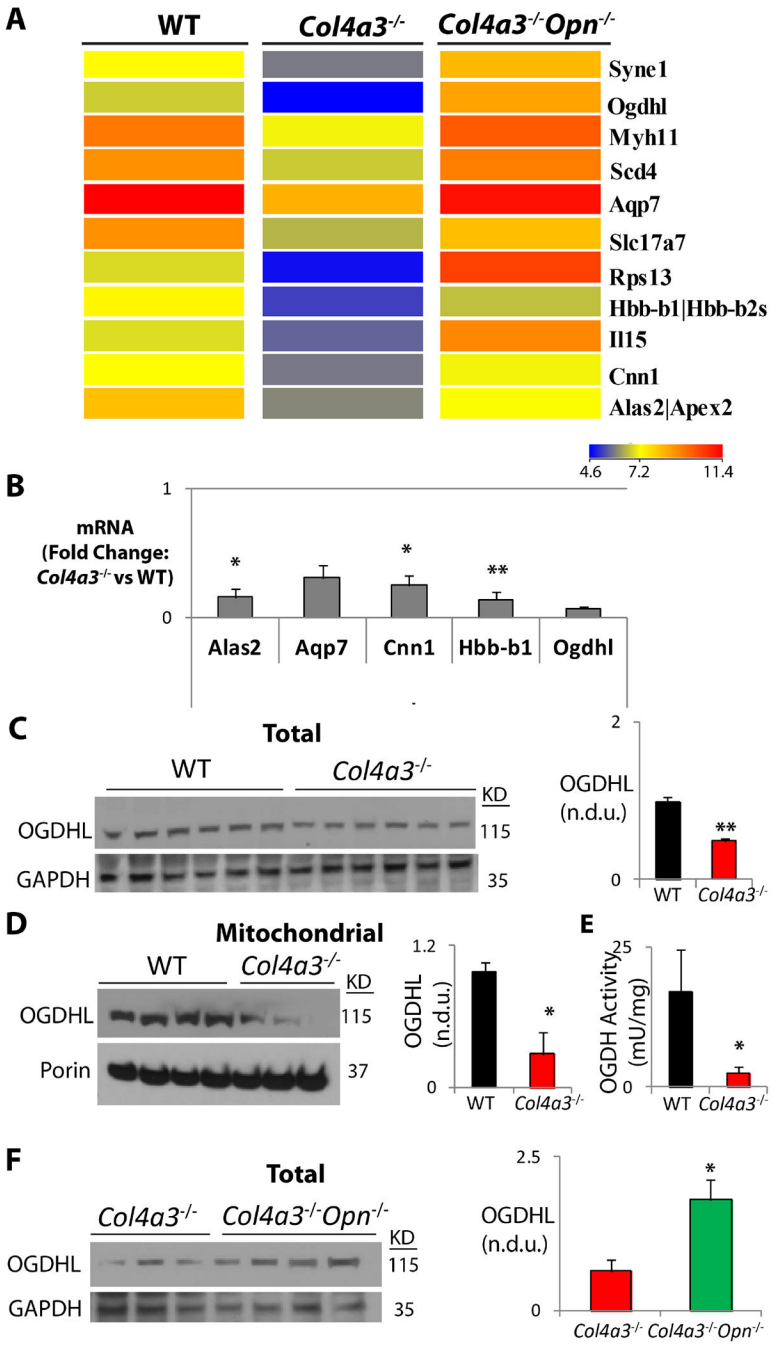

Figure 3: OGDHL is dysregulated in *Col4a3*$^{-/-}$ hearts and normalized by OPN deficiency.

A. Microarray heatmap shows genes that are altered in the *Col4a3*$^{-/-}$ hearts and upregulated with OPN deficiency. **B.** The downregulation of selected genes in the *Col4a3*$^{-/-}$ hearts is validated by qPCR. Target validation in whole heart tissue **(C)** or mitochondrial fraction **(D)** shows reduced OGDHL protein and suppressed OGDH activity **(E). F.** OGDHL protein levels are upregulated with OPN knockout in the *Col4a3*$^{-/-}$ hearts. Data are mean±SEM. N=3–5 hearts per group. *p<0.05 and **p<0.01 using unpaired Student's t-test.

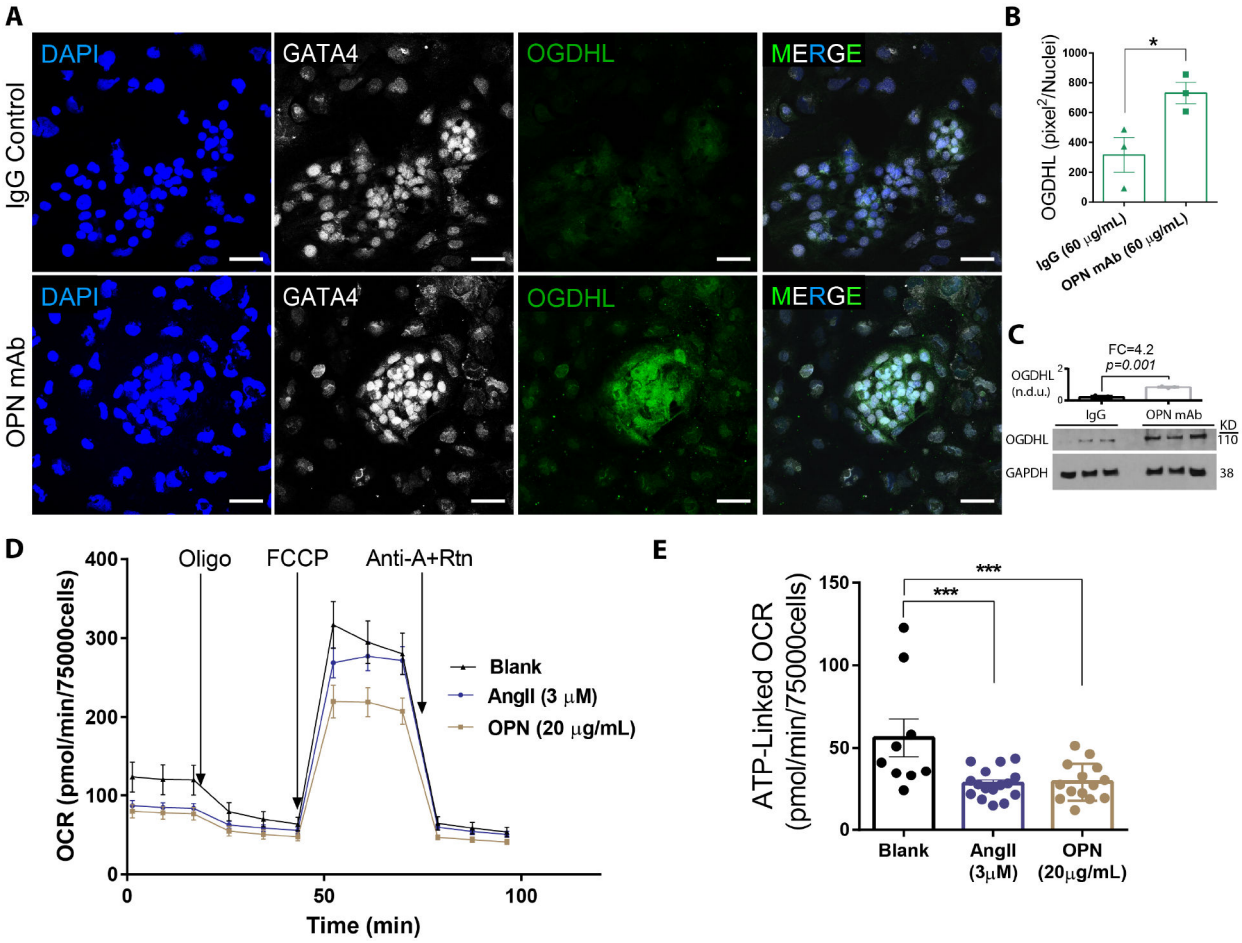

Figure 4: OPN negatively regulates OGDHL in hiPS-CMs and respiration in nCMs.

A-C. Treatment of hiPS-CMs with OPN mAb significantly increases OGDHL protein levels by immunostaining and western blotting. N= 3 wells per group. **D-E.** Mouse neonatal cardiomyocytes treated with 20 μg/ml mouse recombinant OPN for 48 hours show significantly reduced ATP-linked oxygen consumption rate. N=9–16 wells per group. Data are representative of 3 independent experiments. Data are mean±SEM. *p<0.05, **p<0.01, ***p<0.001 using unpaired Student's t-test.

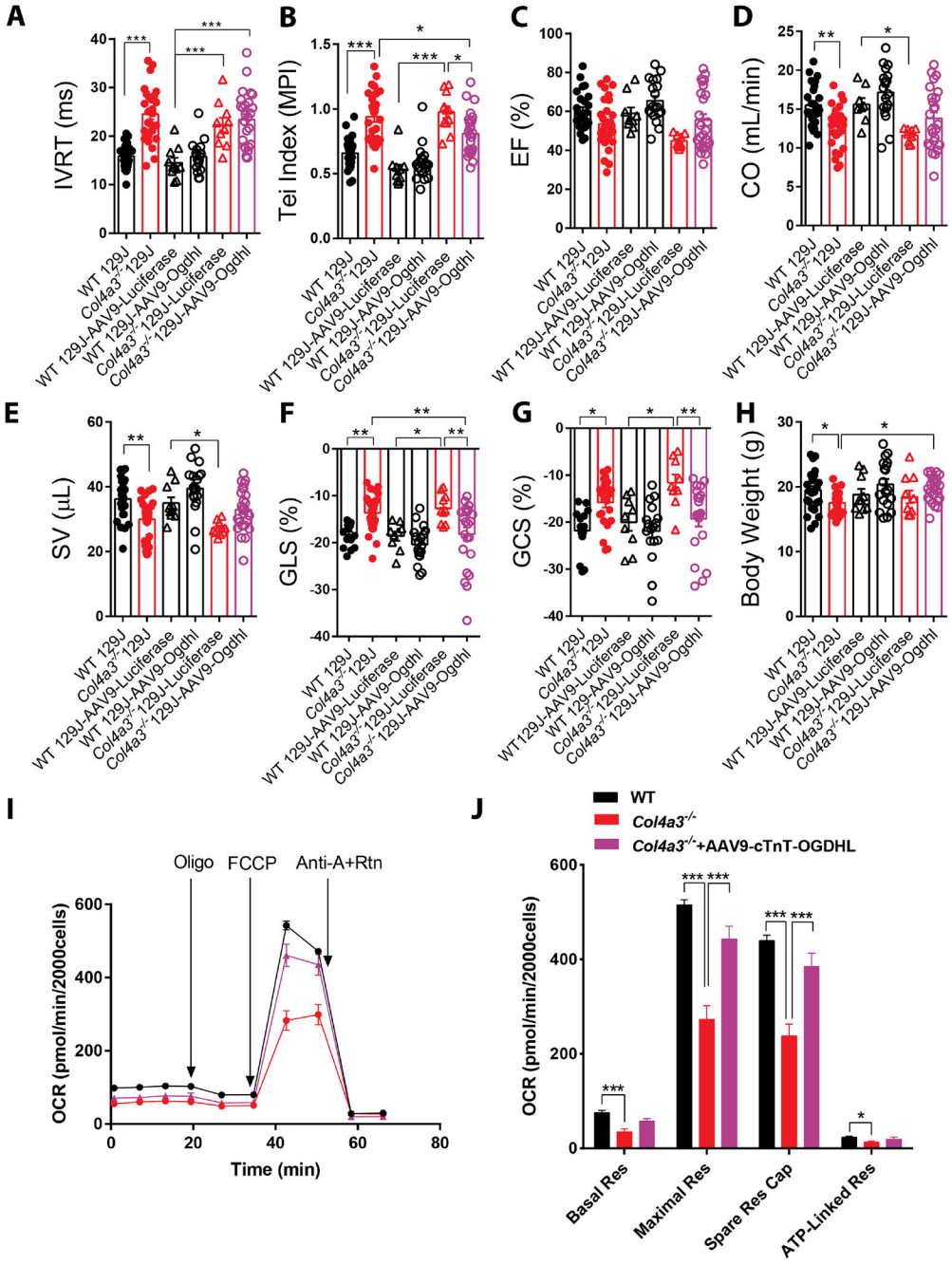

Figure 5: Cardiac dysfunction and impaired mitochondrial function in *Col4a3*$^{-/-}$ mice are rescued by heart-specific Ogdhl overexpression.

A-G Cardiac function of *Col4a3*$^{-/-}$ 129J mice was evaluated by echocardiography and strain analysis four weeks after AAV9-cTnt-Ogdhl or AAV9-cTnt-Luciferase injections showing improved MPI **(B)**, improved strain **(F,G)** and reduced weight loss **(H).** Complete echocardiographic and morphometric measurements are presented in Online Tables 4 and 5. **I-J**. Extracellular flux assay confirmed suppressed mitochondrial respiration in adult cardiomyocytes isolated from *Col4a3*$^{-/-}$ hearts. Four weeks post AAV9-cTnt-Ogdhl injections, the adult myocytes show significantly improved oxygen consumption rate (OCR).

Data are mean±SEM. N=15–29 mice per group. *p<0.05, **p<0.01, ***p<0.001 using one-way ANOVA with Tukey's post hoc test.

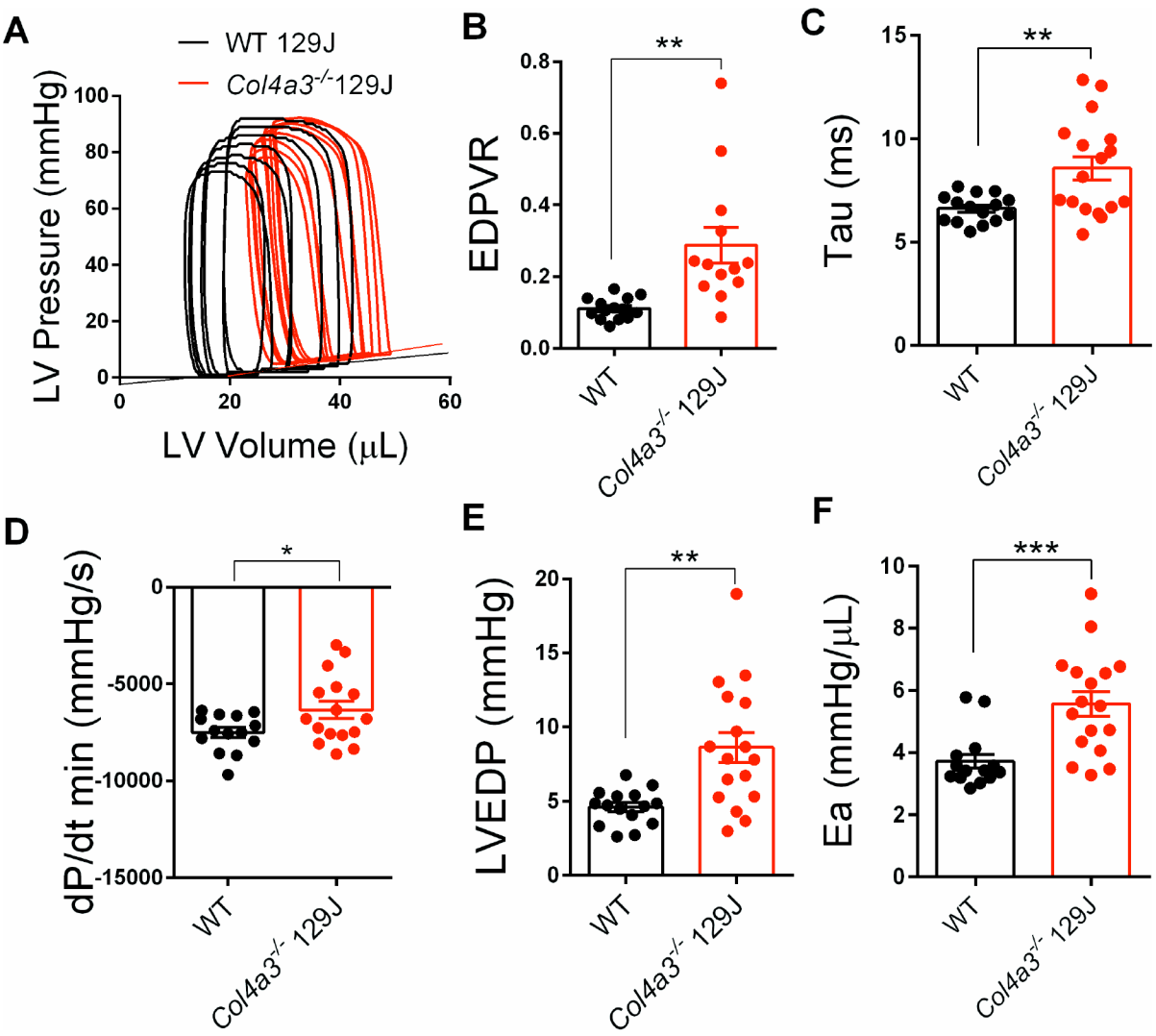

Figure 6: Pressure Volume Analysis of *Col4a3*$^{-/-}$ 129J mice.

Invasive hemodynamic measurements demonstrated that 2-month *Col4a3*$^{-/-}$ 129J background mice develop diastolic dysfunction. Complete invasive hemodynamic measurements are presented in Online Table 6. Data are mean±SEM. N=13–18 mice per group. *p<0.05, **p<0.01, ***p<0.001 using unpaired Student's t-test.

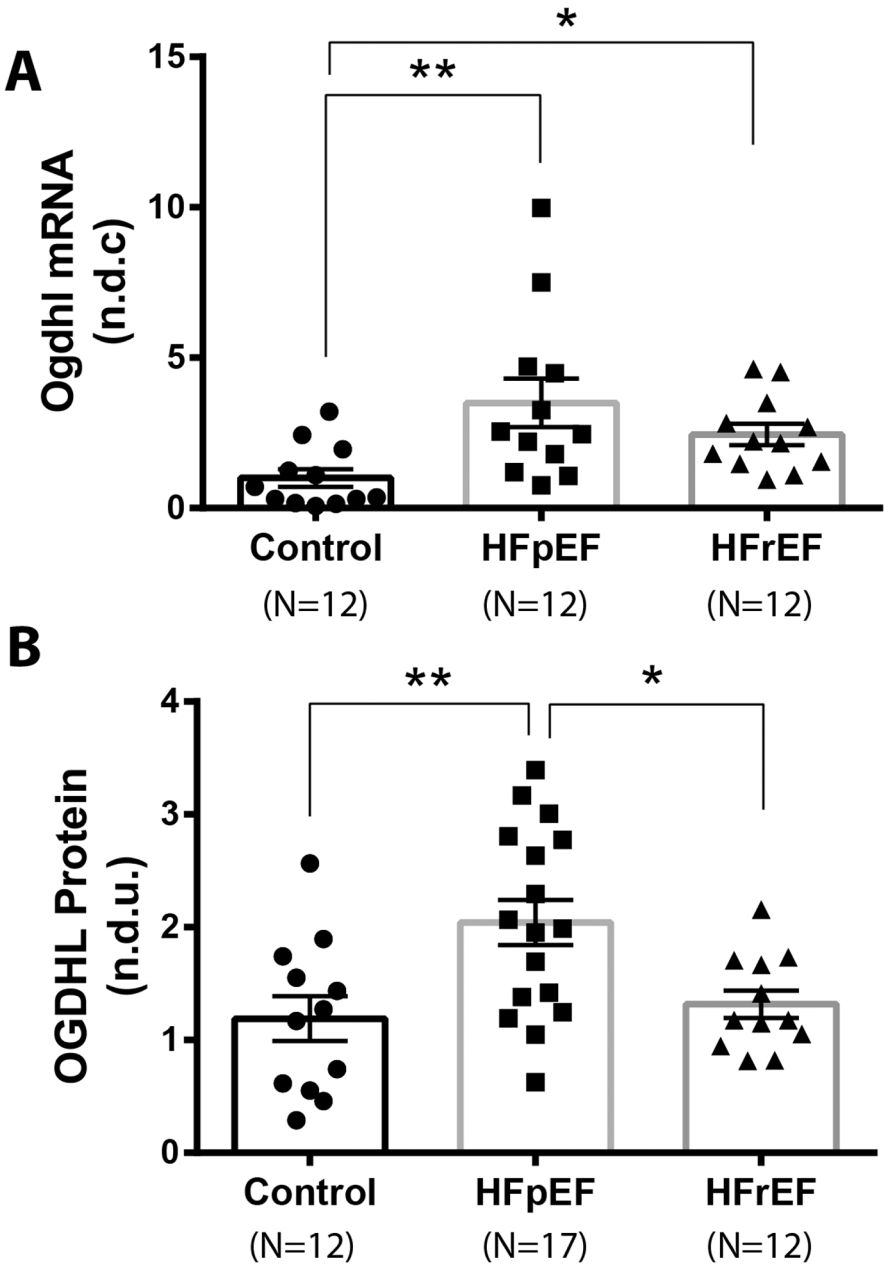

Figure 7: OGDHL expression is dysregulated in cardiac biopsies of HFpEF patients.

Ogdhl mRNA **(A)** and protein **(B)** levels are upregulated in HFpEF patients as shown by qPCR and western blotting, respectively. n.c.u.: Normalized Delta C, n.d.u.: Normalized Densitometry Unit. Data are mean±SEM. N=12–18 per group. *p<0.05, and **p<0.01, using Kruskal-Wallis nonparametric test with Dunn's multiple comparisons test for qPCR and one-way ANOVA with Holm-Sidak's post hoc test for western blots.

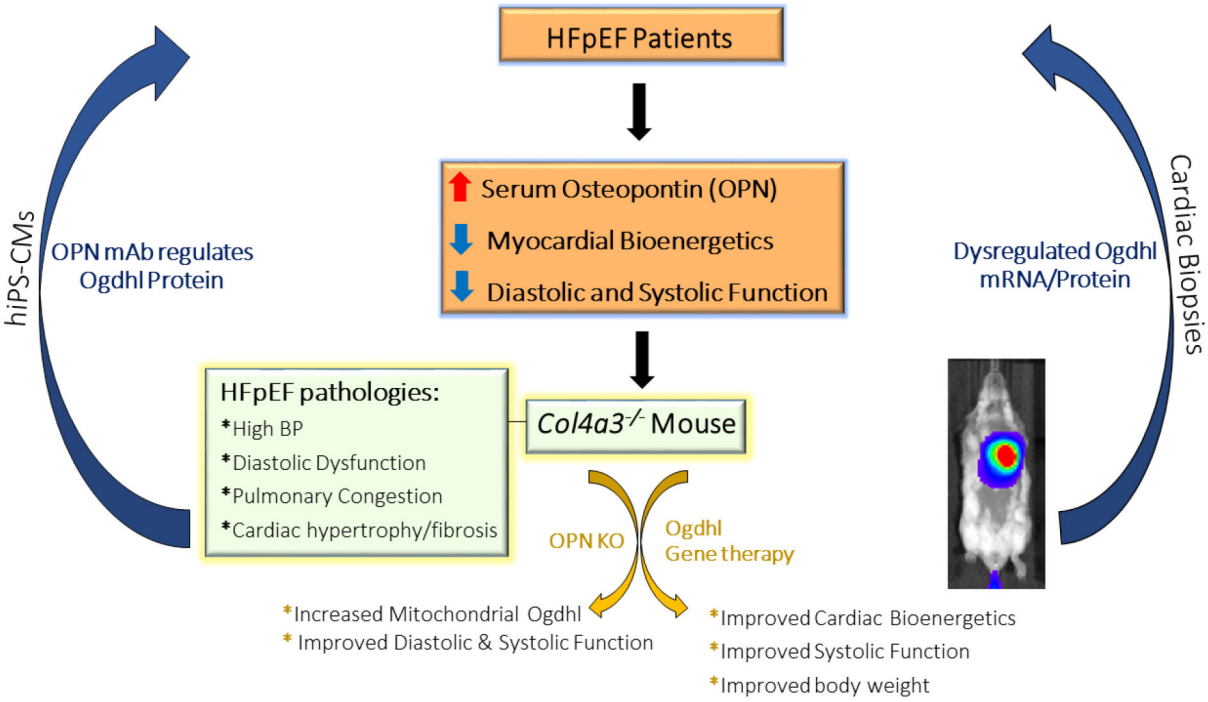

Central Illustration: Osteopontin and Mitochondrial OGDHL in Diastolic Dysfunction.
The phenotype of a subset of patients with HFpEF including a possible central and causative role for Osteopontin (OPN) is mimicked in Alport (*Col4a3*$^{-/-}$) mice. Our studies show that OPN regulates mitochondrial 2-Oxoglutarate Dyhydrogenase (OGDHL) and myocardial bioenergetics in a preclinical model, and this at least partially drives the HFpEF phenotype. The results were validated in human induced pluripotent-derived cardiomyocytes (hiPS-CMs), and cardiac biopsies of HFpEF patients.

Table 1.

Patient demographics.

	ALL			RNA			Protein		
	Control (18)	**HFpEF (27)**	**HFrEF (19)**	**Control (12)**	**HFpEF (12)**	**HFrEF (12)**	**Control (12)**	**HFpEF (17)**	**HFrEF (12)**
Age (years)	57	63	57	60	64	58	57	63	59
% Female	50	56	32	50	67	8	42	47	50
% Caucasian	83	26	74	75	25	67	92	24	83
% ACE-I or ARB	17	59	63	25	67	67	0	53	67
% BB	17	67	95	25	83	92	8	59	100
% Insulin	6	37	16	0	50	8	8	35	17
% Diuretic	0	96	100	0	100	100	0	94	100
% HTN	39	96	100	50	100	100	25	94	100
% DM	17	63	21	17	67	17	8	65	17
% CAD	6	11	11	8	17	17	0	12	0
% Afib	6	30	58	8	33	50	0	29	83
BMI (kg/m2)	26.4	39.9	26.0	26.4	36.5	26.2	26.8	41.6	25.8
RAP (mmHg)		11	7		12	7		11	7
PCWP (mmHg)		19	18		20	17		18	19
CI (L/m/m2)		2.46	2.20		2.43	2.40		2.43	2.05
LVEF (%)	60	65	17	60	65	17	60	65	16